$GABA_A$ Receptor Deficits Predict Recovery in Patients With Disorders of Consciousness: A Preliminary Multimodal [^{11}C]Flumazenil PET and fMRI Study

Pengmin Qin,[1,2,3] Xuehai Wu,[4] Niall W. Duncan,[1,2,3,5] Weiqi Bao,[6] Weijun Tang,[7] Zhengwei Zhang,[6] Jin Hu,[4] Yi Jin,[4] Xing Wu,[4] Liang Gao,[4] Lu Lu,[8] Yihui Guan,[6] Timothy Lane,[2,3] Zirui Huang,[2] Yelena G. Bodien,[9] Joseph T. Giacino,[9] Ying Mao,[4]* and Georg Northoff[1,2,3,5,10]*

[1]Graduate Institute of Humanities in Medicine, Taipei Medical University, Taipei, Taiwan
[2]Institute of Mental Health Research, University of Ottawa, Ottawa, Canada
[3]Brain and Consciousness Research Centre, Taipei Medical University-Shuang Ho Hospital, New Taipei City, Taiwan
[4]Neurosurgery Department, Huashan Hospital, Fudan University, Shanghai, China
[5]Centre for Cognition and Brain Disorders (CCBD), Hangzhou Normal University, Hangzhou, China
[6]PET/CT Centre, Huashan Hospital, Fudan University, Shanghai, China
[7]Radiologic Department of Huashan Hospital, Fudan University, Shanghai, China
[8]Antai Hospital, Shanghai, China
[9]Spaulding Rehabilitation Hospital, Charlestown, Massachusetts
[10]Research Centre for Mind, Brain and Learning, National Chengchi University, Taipei, Taiwan

Abstract: *Objectives:* Disorders of consciousness (DoC)—that is, unresponsive wakefulness syndrome/vegetative state and minimally conscious state—are debilitating conditions for which no reliable markers of consciousness recovery have yet been identified. Evidence points to the GABAergic system being altered in DoC, making it a potential target as such a marker. *Experimental design:* In our preliminary study, we used [^{11}C]Flumazenil positron emission tomography to establish global $GABA_A$ receptor binding potential values and the local-to-global (LTG) ratio of these for specific regions. These values were then compared between DoC patients and healthy controls. In addition, they were correlated with behavioral improvements for the patients between the time of scanning and 3 months later. Functional magnetic resonance imaging resting-state functional connectivity was also calculated

Additional Supporting Information may be found in the online version of this article.

Contract grant sponsor: CIHR, HDRF, EJLB-CIHR, and the Michael Smith Foundation (to G.N.); Contract grant sponsor: National Science Foundation of China; Contract grant number: 31471072 (to N.W.D.); Contract grant sponsor: The National Science Foundation for Distinguished Young Scholars of China; Contract grant number: 81025013 (to Y.M.)

*Correspondence to: Dr. Georg Northoff, MD, PhD, FRCP; 1145 Carling Avenue, Room 6467, Ottawa, ON K1Z 7K4. E-mail: georg.northoff@theroyal.ca (or) Dr. Ying Mao; Neurosurgery Department, Shanghai Huashan Hospital, Fudan University, Shanghai, China. E-mail: maoying@fudan.edu.cn
Pengmin Qin and Xuehai Wu contributed equally to the manuscript.

Received for publication 28 March 2015; Revised 5 June 2015; Accepted 12 June 2015.
DOI: 10.1002/hbm.22883
Published online 00 Month 2015 in Wiley Online Library (wileyonlinelibrary.com).

and the same comparisons made. *Principal observations:* lobal $GABA_A$ receptor binding was reduced in DoC, as was the LTG ratio in specifically the supragenual anterior cingulate. Both of these measures correlated with behavioral improvement after 3 months. In contrast to these measures of $GABA_A$ receptor binding, functional connectivity did not correlate with behavioral improvement. *Conclusions:* Our preliminary findings point toward $GABA_A$ receptor binding being a marker of consciousness recovery in DoC. *Hum Brain Mapp 00:000–000, 2015.*

Key words: vegetative state; minimally conscious state; functional connectivity; unresponsive wakefulness syndrome; Zolpidem; salience network; default-mode network; executive-control network

INTRODUCTION

Unresponsive wakefulness syndrome (UWS; formerly known as vegetative state) and minimally conscious state (MCS) are debilitating neurological conditions characterized as disorders of consciousness (DoC). For patients with DoC, early prognosis and therapy are crucial but markers of recovery are presently lacking.

A number of lines of evidence suggest that the GABAergic system could be a possible target for identifying such markers. First, GABAergic substances such as Zolpidem, a $GABA_A$ receptor agonist [Salva and Costa, 1995], appear to be therapeutically efficacious in a subset of UWS and MCS patients [Chatelle et al., 2014; Ciurleo et al., 2013; Clauss, 2011; Pistoia et al., 2010; Rodriguez-Rojas et al., 2013; Thonnard et al., 2014]. Second, an early positron emission tomography (PET) study showed reductions in $GABA_A$ receptors across the whole brain in nine patients with UWS [Rudolf et al., 2000]. Unfortunately, this study did not address specific regional deficits or recovery prognosis [Laureys et al., 2000] and has not been followed up in any subsequent investigations of $GABA_A$ receptors in DoC.

Recent studies have identified altered resting-state functional magnetic resonance imaging (fMRI) activity in various brain networks in patients with DoC, including the salience network (SN), the default-mode network (DMN), and the executive-control network (ECN) [Crone et al., 2013; Demertzi et al., 2014; Qin et al., 2010; Thonnard et al., 2013]. These networks, therefore, represent plausible targets to focus any investigation of $GABA_A$ receptors on. The SN may be of particular interest as fMRI activity levels in a subcomponent of that network—the supragenual anterior cingulate cortex (SACC)—induced by the presentation of the patient's name predicted clinical outcomes in DoC [Qin et al., 2010]. In addition, Zolpidem administration was seen to increase activity within the ACC (and orbitofrontal cortices), with concurrent transient improvements in motor and cognitive performance in one patient with akinetic mutism [Brefel-Courbon et al., 2007]. Zolpidem administration has also been shown to increase metabolism (as measured with [18F]flurodeoxyglucose PET) in the mesiofrontal and dorsolateral prefrontal cortices in three MCS patients [Chatelle et al., 2014]. All three patients recovered functional communication after Zolpidem administration, highlighting the potential of the GABAergic system as a prognostic marker.

Given the potential importance of GABAergic changes in DoC, one might hypothesize that measures of $GABA_A$ receptors in the brain, and in particular in the ACC, can predict recovery in DoC. To test this, we measured $GABA_A$ receptor binding using [^{11}C]flumazenil PET, along with resting-state fMRI. Although the available sample size ($n = 12$ UWS and MCS) makes this study preliminary, this multimodal approach is unique in DoC patients.

METHODS

Participants

Seventeen patients with DoC (11 UWS and 6 MCS) were recruited. None were taking benzodiazepines at the time of scanning, nor in the 3 months prior [Guadagno et al., 2008]. Five patients (four UWS, one MCS) who required sputum aspiration during the PET scan were excluded from the analysis, leaving 12 DoC patients (seven UWS, five MCS; four female; mean age = 45.6 years [±3.3 SD]; age range = 23–61 years; time post injury range = 36–233 days; see Table I for patient details).

Diagnosis of UWS or MCS was made according to the Coma Recovery Scale-Revised (CSR-R) [Giacino et al., 2004] by an experienced physician (XW) who was not involved in the analysis of the data. The CRS-R comprises six subscales addressing auditory, visual, motor, oromotor/verbal, communication, and arousal components, reflecting the level of consciousness in the patient's behavior. Patients were assessed on the day before the PET session and reassessed immediately prior to the PET scan (T0). Importantly, the two assessments showed consistent results for all patients. All patients were then reassessed 3 months after PET scanning (T1). This reassessment was based on CRS-R scores from two separate examinations within 1 week of each other (giving consistent scores for all patients). The difference between CSR-R scores at T1 and T0 was taken as a measure of behavioral change for the patients (i.e., T1 minus T0, where a positive score represents a behavioral improvement). Three patients who showed behavioral improvements at T1 were rescanned; however, the data from only one of these patients were

TABLE I. Patient clinical information

Patient	Age/sex	Time since brain injury (days)	Cause	Lesions on MRI	PET scanning (T0)		3 months later (T1)	
					CRS-R	Diagnosis	CRS-R	Diagnosis
MCS-1	36/M	38	TBI	Bilateral frontal cortex	7	MCS	23	EMCS
MCS-2	51/M	229	SIH	Brain stem and left basal ganglia, left thalamus	9	MCS	9	MCS
MCS-3	54/M	111	TBI	Bilateral temporal cortex and bilateral frontal cortex, brain stem	10	MCS	10	MCS
MCS-4	50/M	64	TBI	Bilateral temporal cortex, left occipital cortex, left basal ganglia, left parietal cortex, right thalamus, and brain stem	6	MCS	14	MCS
MCS-5	42/M	36	TBI	Bilateral frontal cortex	7	MCS	23	EMCS
UWS-1	61/F	225	TBI	Bilateral frontal and temporal cortex, brain stem	6	UWS	6	UWS
UWS-2	58/M	194	TBI	Bilateral frontal and temporal cortex, right occipital cortex, brain stem	4	UWS	4	UWS
UWS-3	37/M	47	TBI	Bilateral frontal cortex, right temporal and occipital cortex, brain stem	5	UWS	5	UWS
UWS-4	23/F	233	TBI	Left thalamus and brain stem	6	UWS	6	UWS
UWS-5	58/F	98	SIH	Bilateral frontal and temporal cortex, right thalamus and brain stem	6	UWS	–	–
UWS-6	43/F	47	TBI	Right temporal cortex and right thalamus, brain stem	5	UWS	23	EMCS
UWS-7	35/M	115	TBI	Right temporal and occipital cortex, bilateral frontal cortex, brain stem	7	UWS	21	EMCS

Note: EMCS = emergence from minimally conscious state. "–" denotes unavailable information. TBI = traumatic brain injury; SIH = spontaneous intracerebral haemorrhage.

usable as the other two patients felt discomfort in the scanner and so could not complete the data acquisition.

Nine healthy volunteers participated in the study (four female; mean age = 35.6 years [±4.06 SD]; age range = 23–55 years). There was no age difference between patients and healthy controls (HC) ($P = 0.07$). None of the healthy participants had a history of neurological or psychiatric disorders or were taking medication. Two of these HC were rescanned 3 months after their initial one (i.e., at T1). Written informed consent was obtained from the healthy participants and the legal representatives of the patients. The study was approved by the Ethics Committees of the Shanghai Huashan Hospital, Fudan University, Shanghai, China.

GABA$_A$ Receptor Binding Potentials

PET imaging with radiolabeled flumazenil (FMZ), a benzodiazepine antagonist that binds at the GABA$_A$ receptor benzodiazepine site, has been widely used to measure GABA$_A$ receptor density in vivo in humans [Frey et al., 1991]. Whole-brain [11C]FMZ data was obtained using a Siemens Biograph 64 positron emission tomography-computed tomography (PET/CT). Head movement was minimized with a head-restraining adhesive band. A CT scan was acquired for attenuation correction, followed by an intravenous tracer injection (over 60 s) of 380.3 MBq (±70.4 SD) of [11C]FMZ for HC and 386.0 MBq (±70.0 SD) of [11C]FMZ for patients. Doses did not differ between patients and healthy subjects (independent two-sample t-test, $t = 1.86$, $P = 0.85$). Participants were instructed to close their eyes and remain awake during scanning. To ensure that healthy participants remained awake during scanning, they were asked to raise their hand every 10 min. Similar prompts were given to patients, as has been done in previous studies [Demertzi et al., 2014; Vanhaudenhuyse et al., 2010].

Three-dimensional (3D) list-mode data were acquired for a period of 60 min and then binned into a series of 26 frames consisting of six 30-s frames followed by seven 60-s, five 120-s, and eight 300-s frames [Salmi et al., 2008]. A linear 3D filtered backprojection (3D-FBP) was preferred for the modeling analysis of [11C]FMZ kinetics [van Velden et al., 2009] with full accounting for scatter, random

coincidences, attenuation, decay dead-time correction, and frame-based motion correction [Costes et al., 2009]. The in-plane reconstructed resolution was 6-mm full-width at half-maximum. The images used had a voxel size of 1.22 × 1.22 × 1.22 mm^3 (256 × 256 × 207 voxels). We used a subset from 10 to 60 min to calculate the binding potential (BP_{ND}) according to the Logan plot method [Logan et al., 1996]. The bilateral cerebellar white matter was used as the reference as it generally has less damage than other brain regions in DoC patients [Qin et al., 2012; Rudolf et al., 2000] (see Supporting Information Fig. 1 for patient cerebellar structural images). To define this reference region, each person's T1-weighted 3D anatomical MRI image (see MRI Data Acquisition and Processing for details) was segmented using the FAST tool from FSL to give a white matter map and then aligned to their binding potential image. The white matter maps were masked with the cerebellar mask from the Harvard Oxford atlas (http://fsl.fmrib.ox.ac.uk/fsl/fslwiki/Atlases), thresholded at 0.9 (from a range of 0 to 1), and binarized. The resulting cerebellar white matter mask was then eroded by one voxel to generate the final individual reference region.

Regions of Interest

Using the AFNI template (TT_desai_dk_mpm) [Desikan et al., 2006], we defined regions of interest (ROIs) corresponding to the functional networks identified in previous studies as showing altered activity in DoC [Crone et al., 2013; Demertzi et al., 2014; Qin et al., 2010; Thonnard et al., 2013]. These were the SN, the DMN, the ECN, and the auditory network (AN). The SN ROI was composed of the SACC and anterior insula (AI); the DMN of the posterior cingulate cortex (PCC), perigenual anterior cingulate cortex (PACC), and bilateral temperoparietal junction (TPJ); and the ECN of the bilateral dorsolateral prefrontal cortex (DLPFC), bilateral inferior parietal lobe (IPL), and precuneus (PreCu). The AN included the bilateral auditory cortex. As the AFNI template does not include a separate AI mask, we created the insula ROI by combining the ventral and dorsal AI regions identified by Deen et al. [2011]. To obtain the individual ROIs for each participant, the BP_{ND} map of each participant (HC and patients) was normalized to a standard T1-weighted template, as described previously [Duncan et al., 2013]. The inverse of these normalization parameters were then used to warp the relevant ROIs from the AFNI template onto the nonnormalized individual BP_{ND} maps for healthy and patient groups [Qin et al., 2010].

Calculating BP_{ND} in Gray Matter

As the $GABA_A$ receptor is predominantly located in the gray rather than white matter [Heiss and Herholz, 2006], and because BP_{ND} is known to correlate with gray matter density [Duncan et al., 2013], it is necessary to limit the ROIs to gray matter only. Were the whole ROI (including both gray and white matter) to be used, any results could be attributed to differences in the volume of gray matter within the particular region between participants rather than differences in $GABA_A$ receptors per se. We, therefore, calculated BP_{ND} in gray matter alone as follows: MRI anatomical images were segmented to give gray matter maps. These were thresholded at 0.5 to create a mask of high-probability gray matter voxels and converted into PET space. To remove additional nontissue voxels, we also thresholded the BP_{ND} maps at 0.5 and applied this mask to the gray matter mask (see Supporting Information Fig. 1 for an example mask). Network ROIs in PET space created previously were then restricted according to these gray matter masks. Finally, the mean $GABA_A$ receptor BP_{ND} within each ROI and within the gray matter as a whole was calculated. To correct for unspecific gray matter volume effects, the mean $GABA_A$ BP_{ND} for each region was divided by the mean gray matter proportion of that region [Qin et al., 2012]. This was done for each network ROI and for the total gray matter region.

Statistical Analysis for PET

For whole-brain BP_{ND} values difference between DoC and HC, the effect of age and FMZ dose were removed from the whole-brain BP_{ND} values using linear regression. The resulting residuals for the whole-brain BP_{ND} values were then compared between DoC patients and HC through a Mann–Whitney *U* test. For the relationship between whole-brain BP_{ND} and CRS-R scores, the effect of participant age, the dose of FMZ, and the length of time since the patient's injury were removed from the whole-brain BP_{ND} values and CRS-R scores through linear regression. The Spearman's correlations between the resulting residuals for the global BP_{ND} values and both the CRS-R scores at T0 and the behavioral change (i.e., CRS-R T1-T0) were then calculated. Finally, as the CRS-R is not a purely quantitative measure but also requires particular patterns of scoring for different diagnoses, we further tested the association between BP_{ND} and behavioral improvement by first classifying a patient as improved or not from whether their CRS-R score was higher at T1 than at T0. They were then classified as having a global BP_{ND} value within or outwith two standard deviations of the mean for healthy participants. The correlation between these classifications was then established through a Fisher's exact test. This classification approach has the additional advantage of potentially providing information that is directly clinically relevant.

Having investigated whole-brain BP_{ND} values, we then focused on these values for particular networks. For this, the BP_{ND} local-to-global (LTG) ratio was calculated for each network and this value used in the subsequent calculations [Qin et al., 2012]. This value represents the mean BP_{ND} in each network divided by the average BP_{ND} of the whole

brain, allowing us to measure potentially differential changes in specific regions relative to the global value and so increase specificity by eliminating global effects. This division may also eliminate the potential effect of age, FMZ dose, and length of time since injury on $GABA_A$ BP_{DN} values [Yamauchi et al., 2005]. Differences between patient and control LTG ratios were tested through Mann–Whitney *U* tests. Bonferroni correction for the four networks was done in each of these comparisons (SN, DMN, ECN, and AN) ($P < 0.05$; $P < 0.0125$ uncorrected).

Finally, following the network level analysis, we investigated the various constitutive brain regions within any of the networks that showed a difference in FMZ BP_{ND} LTG ratio between patients and controls. We repeated the same analysis in each subregion as was done for the network as a whole. In addition, Spearman correlations between network LTG ratios and CRS-R scores at T0 and the behavioral change (T1-T0) were also calculated. Within the specific network, Bonferroni correction was done based on the number of brain regions constituting it.

MRI Data Acquisition and Processing

Of the 12 patients with usable PET data, 10 also had fMRI data available. All HC had usable fMRI data. MR images were acquired on a Siemens 3 Tesla scanner. Functional images were acquired using a T2*-weighted echo-planar imaging sequence (repetition time/echo time/θ = 2,000 ms/35 ms/90°, field of view = 256 mm, matrix = 64 × 64, slice thickness = 4 mm, gap = 0 mm, 33 slices, 200 volumes). A T1-weighted high-resolution 3D whole-brain image was also obtained (repetition time = 2300 ms, echo time = 2.98 ms, Matrix = 256 × 256, slice thickness = 1 mm). fMRI imaging was done randomly either before or after the PET scan (mean duration between scans = 8.1 days ± 8.9 SD). The diagnoses remained the same for all patients during both fMRI and PET scanning. All the participants (HC and patients) were instructed to close their eyes and remain awake during scanning. Unfortunately, due to their condition, it was not possible to entirely ensure wakefulness in the patients [Demertzi et al., 2014].

The data were processed using the AFNI and FSL software packages. The first two volumes were discarded. The data then underwent a preprocessing procedure that included slice-timing correction, two- and three-dimensional head-motion corrections, masking for the removal of the skull, and spatial smoothing using a 6-mm full-width at half-maximum kernel. Time-series were then normalized by computing the ratio of the signal in each voxel and each time point to the mean across all time points, multiplied by 100. The estimated head motion and the mean time-series from the white matter and the cerebrospinal fluid (where these regions were defined using thresholds of 0.99 for each tissue type) were regressed out of the data [Saad et al., 2012]. The data were band-pass filtered, reserving signals between 0.01 and 0.08 Hz [Song et al., 2011].

As minor group differences in head motion can cause spurious differences in imaging measures between them [Power et al., 2012; Van Dijk et al., 2012], a rigorous approach to head-motion correction was adopted. Motion was quantified as the absolute Euclidean distance moved from the head position in the prior time point, as calculated from the six rigid-body motion parameters. Where there was movement of more than 0.5 mm between time points, the relevant volume, plus the preceding and subsequent volumes, was removed from the dataset [Huang et al., 2013]. To obtain reliable functional connectivity values, participants with less than 3 min of data remaining following this procedure were excluded [Yan et al., 2013]. This resulted in the exclusion of three patients (from 10).

We explored the resting-state functional connectivity between the different regions that compose the SN (the AI and the SACC). This network was chosen for the analysis as it was the only one that shows a difference in FMZ BP_{ND} LTG ratio between patients and controls. Considering the similar time course in the corresponding regions between the two hemispheres, and to reduce physiological and scanner noise, we collapsed the time courses from the bilateral AI. Pearson's correlation coefficient between the time-series of AI and SACC was calculated and converted to normally distributed *Z*-values using Fisher's Z transformation. These *Z*-values were compared between patients and controls using a Mann–Whitney *U* test. Finally, we calculated the Spearman correlation between functional connectivity and CRS-R scores at T0, as well as the behavioral change (CRS-R T1 –T0). The significance level was set at $P < 0.05$.

RESULTS

Behavioral and Clinical Data

Five patients showed clear behavioral improvements between T0 and T1 (MCS 1, 4, 5 and UWS 6, 7). MCS 1, 5 and UWS 6, 7 could perform verbal communication 3 months after the initial assessment (Table I, plus Supporting Information Tables I and II). Although MCS 4 was unable to verbally communicate in a stable fashion, they were able to say intelligible words, pursue a visual stimulus, and localize noxious stimulation at T1 (they was unable to do these at T0). The remaining patients did not show any behavioral changes between T0 and T1.

Whole-Brain $GABA_A$ Receptor BP_{ND}

Mean whole-brain $GABA_A$ receptor BP_{ND} values were significantly lower (37% reduction) in DoC patients than in HC ($P = 0.001$) (Fig. 1B). There was a positive correlation between $GABA_A$ receptor BP_{ND} and behavioral change (CRS-R T1-T0) (rho = 0.62, 95% confidence interval

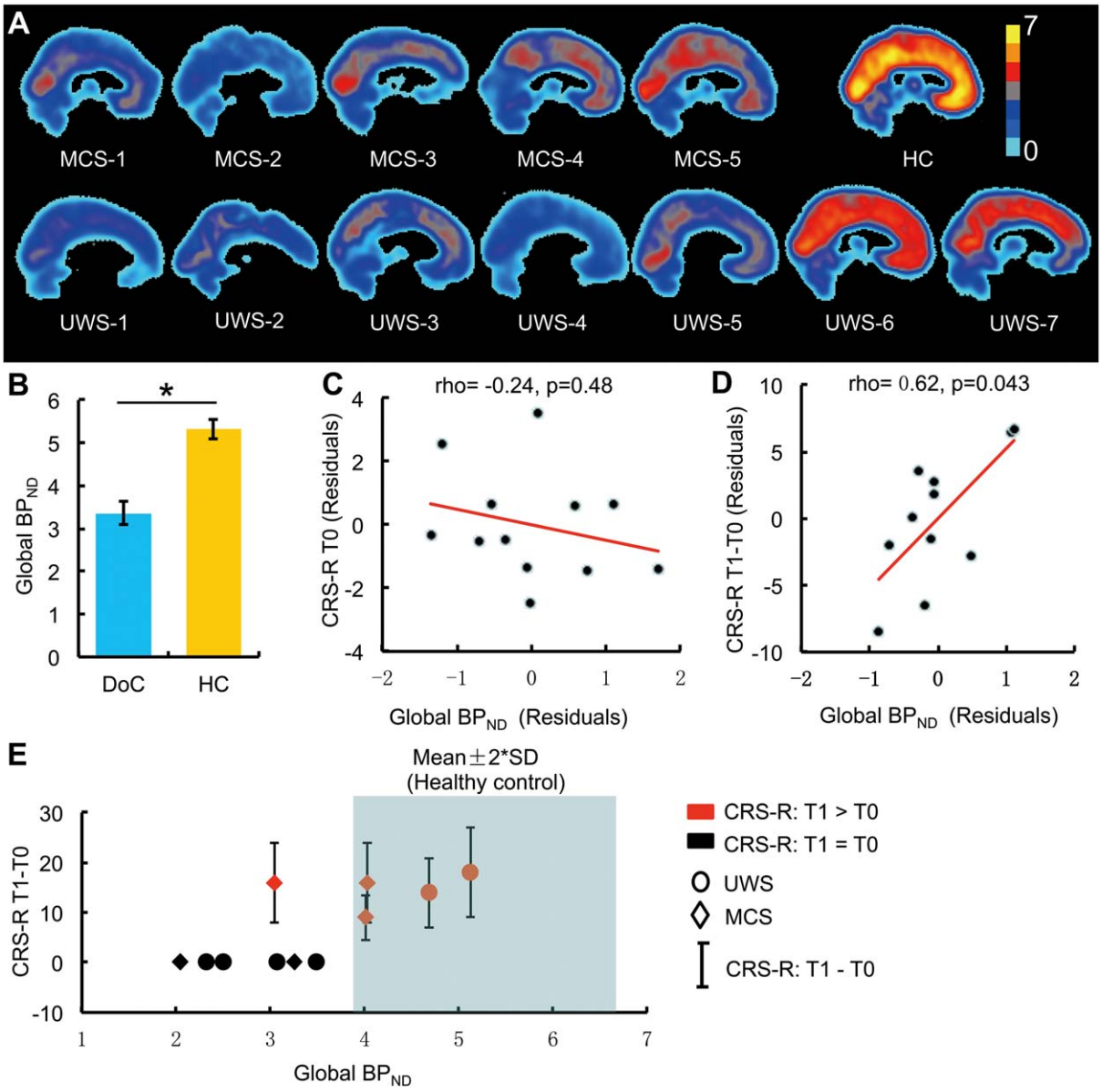

Figure 1.

Global $GABA_A$ receptor BP_{ND}. (**A**) $GABA_A$ receptor BP_{ND} maps from all the patients with DoC and one HC. (**B**) Global $GABA_A$ receptor BP_{ND} values (mean ± SE) for DoC patients and HC. * denotes a significant difference ($P < 0.05$). Spearman correlation between global $GABA_A$ receptor BP_{ND} values and CRS-R scores at (**C**) the time of scanning (T0) and (**D**) CRS-R difference between T1 and T0 (T1-T0). Note that these graphs show residuals after confounding factors (age, FMZ dose, and time since injury) have been regressed out from both global $GABA_A$ receptor BP_{ND} values and CRS-R scores. (**E**) Scatter plot of global $GABA_A$ BP_{ND} values and the difference in CRS-R scores between T0 and T1. The blue shaded area represents the range of mean ± 2*SD of the HC. Note that the bar represents the difference between T0 and T1 and is not shown in the patients who have no difference. The label of either UWS and MCS represents the diagnosis at T0. [Color figure can be viewed in the online issue, which is available at wileyonline library.com.]

[C.I.] = 0.01 − 0.989, $P = 0.043$), but no correlation with CRS-R scores at T0 (Fig. 1 and Supporting Information Fig. 2)

Testing the relationship between behavioral improvement (classed according to whether CRS-R T1 > T0) and BP_{ND} (classed according to whether BP_{ND} values lie within

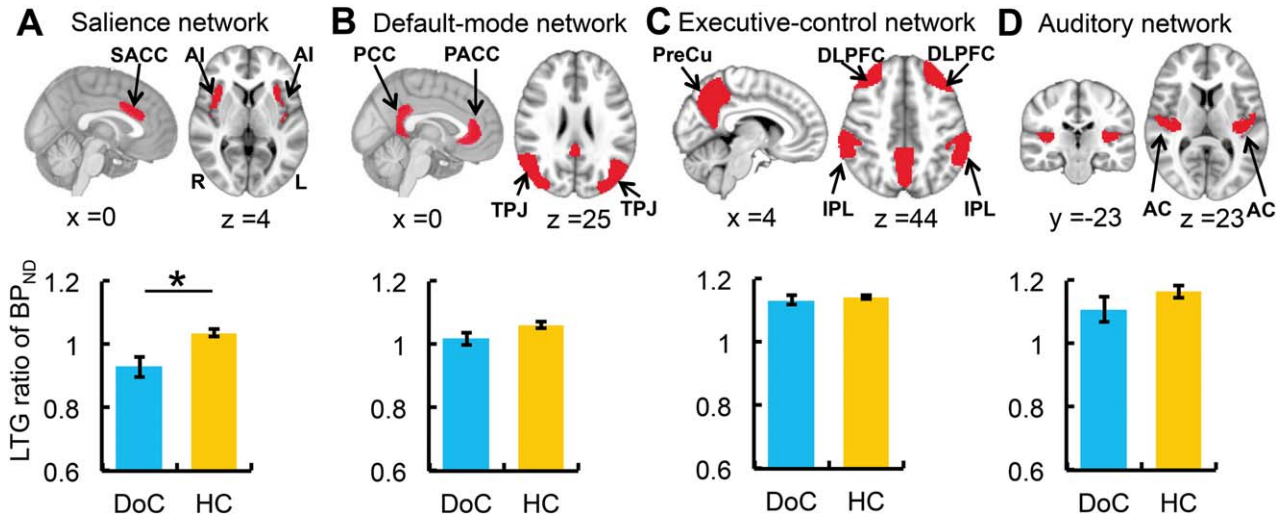

Figure 2.

LTG GABA$_A$ BP$_{ND}$ ratios (mean ± SE) for networks studied in DoC patients and HC. The upper panel shows the regions that make up each network. * denotes a significant difference ($P < 0.05$, corrected). AC = auditory cortex, AI = anterior insula, DLPFC = dorsolateral prefrontal cortex, IPL = inferior parietal lobe, PACC = perigenual anterior cingulate cortex, PCC = posterior cingulate cortex, PreCu = precuneus, SACC = supragenual anterior cingulate cortex, TPJ = temperoparietal junction. [Color figure can be viewed in the online issue, which is available at wileyonlinelibrary.com.]

2 SD of HC mean), a positive correlation was observed (Fisher's exact test, $P = 0.015$) (Fig. 1E). All patients who did not improve between T0 and T1 showed lower GABA$_A$ receptor BP$_{ND}$ than those who had an improvement in their level of consciousness.

Network GABA$_A$ Receptor BP$_{ND}$

Absolute GABA$_A$ receptor BP$_{ND}$ in each of the networks studied (SN, DMN, ECN, and AN) was lower in patients than in HC (Supporting Information Fig. 3). Taking this global reduction into account through LTG ratios, there was a relative reduction in GABA$_A$ receptor BP$_{ND}$ values between patients and HC in the SN specifically ($P = 0.024$ corrected; $P = 0.006$ uncorrected) (Fig. 2). There was no reduction in LTG ratios in the other networks studied. Within the patient group, there was no different in LTG ratios between UWS and MCS patients (Supporting Information Fig. 4 and 5).

GABA$_A$ Receptor BP$_{ND}$ in the SN

With only the SN showing reduced LTG ratios, we investigated this network further by dividing it into its constituent regions—the SACC and the AI. BP$_{ND}$ LTG ratios were significantly reduced in the SACC in patients with DoC when compared with HC ($P = 0.004$ corrected; $P = 0.002$ uncorrected), as were LTG ratios in the AI ($P = 0.036$ corrected; $P = 0.018$ uncorrected) (Fig. 3B).

We then tested the correlation between LTG ratios and behavioral change (CRS-R T1 minus T0) in each region. The LTG in the SACC was significantly correlated with behavioral change (rho = 0.81, 95% C.I. = 0.48 − 0.95, $P = 0.004$ corrected, $P = 0.002$ uncorrected) (Fig. 3C), while no correlation was seen in the AI. However, the relationship between LTG ratio in the SACC (whether LTG ratio lie within 2 SD of HC mean) and behavioral improvement classification (CRS-R T1 > T0) was not significant (Fisher's test, $P = 0.08$) (Fig. 3D).

To establish the specificity of the SACC, we also investigated other areas of the cingulate cortex (Supporting Information Fig. 6). A reduction in LTG ratios in DoC patients was additionally seen in the perigenual anterior cingulate (PACC). There was no change in the mid-cingulate cortex and the PCC. However, there was no correlation between LTG ratios of the PACC and CRS-R scores at T0 or with behavioral change (T1-T0).

BP$_{ND}$ After Behavioral Improvement

UWS6 was scanned at both T0 and T1. Both their global BP$_{ND}$ and LTG ratio in the SACC were located within the range of the HC at T1 (they were also in this range at T0). Two HC also underwent a second scan 3 months after their first. There were no differences in their global BP$_{ND}$ values between these times (Supporting Information Fig. 7).

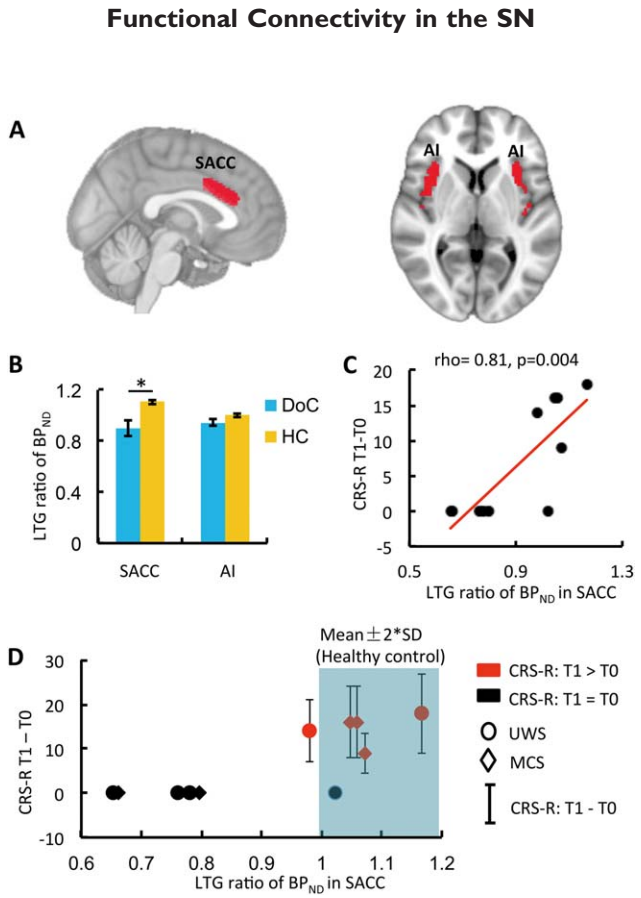

Figure 3.

LTG BP_{ND} ratio in SN. (**A**) Brain regions forming the SN. SACC = supragenual anterior cingulate cortex, AI = anterior insula. (**B**) The LTG BP_{ND} ratio (mean ± SE) for DoC patients and HC in the SACC and AI. * denotes a significant difference ($P < 0.05$, corrected). (**C**) Spearman correlation between the behavioral change (CSR-R T1-T0) and LTG ratio in the SACC. (**D**) Scatter plot of LTG $GABA_A$ BP_{ND} ratios in the SACC and the difference in CRS-R scores between T0 and T1. The blue shaded area represents the range of mean ± 2*SD of the HC. Note that the bar represents the difference between T0 and T1 and is not shown in the patients who have no difference. The label of either UWS and MCS represents the diagnosis at T0. [Color figure can be viewed in the online issue, which is available at wileyonlinelibrary.com.]

Functional connectivity between the SACC and AI (the subregions of the SN) was reduced in patients with DoC, as compared with HC ($P = 0.016$) (Fig. 4). However, unlike with $GABA_A$ receptor BP_{ND}, functional connectivity did not correlate with patients' CRS-R scores at T0, nor with their behavioral change (T1-T0)

Although outwith the focus of our analysis, for completeness, we also looked at functional connectivity in the other networks. Functional connectivity was reduced in each of the DMN, ECN, and AN in DoC patients. Subdividing these networks into their constituent ROIs, in the DMN, functional connectivity was reduced between the PACC and PCC; while in the ECN, functional connectivity was reduced between the DLPFC and PreCu only (Supporting Information Fig. 8).

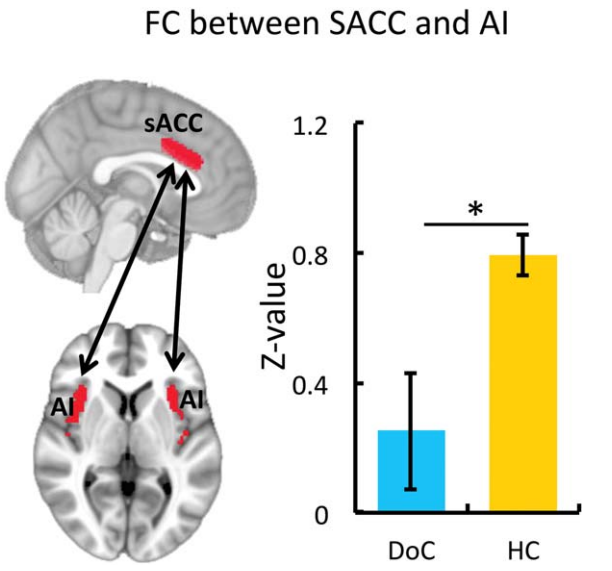

Figure 4.

Functional connectivity (FC) (Mean ± SE) between SACC and AI. Pearson's *r*-values were converted to Fisher's *Z*-values. * denotes $P < 0.05$. [Color figure can be viewed in the online issue, which is available at wileyonlinelibrary.com.]

DISCUSSION

Our preliminary study reports major $GABA_A$ receptor deficits in the whole brain, in the SACC in particular, and in DoC. These GABAergic alterations can predict recovery after 3 months. The potentially special role of the SACC was further supported by alterations in resting-state functional connectivity, as measured with fMRI, in the same patients. Although preliminary, our results demonstrate for the first time that $GABA_A$ receptor BP_{ND} can be linked to outcomes in DoC. Our findings may bear important implications for the understanding of altered GABAergic mechanisms in DoC and point toward use of FMZ PET as a prognostic marker in UWS and MCS.

Global Deficits in $GABA_A$ Receptors and GABAergic Therapy

Our study replicated earlier findings of reduced whole-brain $GABA_A$ receptor binding in UWS [Rudolf et al., 2000] and extended them by providing a link to outcomes. Previous studies suggested that $GABA_A$ receptor changes could reflect irreversible neuronal damage [Heiss, 2012].

This may provide one potential interpretation to the prognostic value of whole-brain $GABA_A$ receptor BP_{ND}. This is supported by the data from the patient scanned at both T0 and T1, where there is no difference in BP_{ND} before and after recovery of consciousness.

GABAergic drugs such as Zolpidem have been shown to restore consciousness in some DoC patients [Ciurleo et al., 2013; Clauss, 2010; Clauss, 2011; Pistoia et al., 2010]. The mechanism of this effect is unknown but may be related to the hypersensitive state of GABA receptors in neurodormant cells [Clauss and Nel, 2006]. It is hypothesized that after brain injury GABA receptors become hypersensitive so that decreased GABA can suppress cellular metabolism and maintain a dormant state. With the introduction of Zolpidem, GABA receptor function may be returned to normal, ceasing the dormant state. Based on our findings, one would predict that the subset of patients who are reactive to Zolpidem [Whyte et al., 2014] might show particularly high degrees of $GABA_A$ receptor binding when compared with those that do not [Ciurleo et al., 2013; Du et al., 2014; Singh et al., 2008].

SN and SACC in DoC

In addition to whole-brain changes, we also showed that there is a reduction in the LTG ratio of $GABA_A$ receptor BP_{ND} in the SN, specifically in the SACC. As with whole-brain BP_{ND}, the SACC LTG ratio was correlated with behavioral improvement after 3 months. The SN, and particularly the SACC, has previously been demonstrated to be associated with consciousness [Crone et al., 2013; Devinsky et al., 1995; Qin et al., 2010]. Moreover, the "mesocircuit hypothesis" for the recovery of consciousness claims a central role for the connection between thalamus and anterior frontal cortex (especially the SACC) in recovery of consciousness [Schiff, 2010]. Our results provide support for this hypothesis by showing a particular relationship between SACC BP_{ND} and the recovery of consciousness.

Functional connectivity between the SACC and the AI was also reduced in patients with DoC. Unlike with SACC BP_{ND}, however, the degree of connectivity was not correlated with the level of consciousness at T1. This suggests that there may be a dissociation in the role that SACC $GABA_A$ receptor binding and functional connectivity play in supporting consciousness. If we consider $GABA_A$ receptor BP_{ND} to reflect neuronal integrity [Heiss, 2012], then, this contrasts with functional connectivity, which instead reflects neural activity synchronization between regions. In DoC patients, the remaining tissue may suffer from a major decrease in metabolism [Laureys and Schiff, 2012; Northoff, 2014; Shulman et al., 2003]. Such a metabolic decrease may put neurons into the aforementioned "dormant state" which may in turn down-modulate functional connectivity [Ciurleo et al., 2013; Du et al., 2014].

Besides the SN, previous studies have also shown reduced functional connectivity within the DMN, ECN, and AN in DoC patients when compared with HC [Demertzi et al., 2014]. This is consistent with our findings of significantly reduced functional connectivity (Supporting Information Fig. 8) and BP_{ND} in these networks (Supporting Information Fig. 3). The reduction in BP_{ND} would appear to reflect a generalized or global effect, as the difference between DoC patients and controls is lost following normalization of the values (i.e., the calculation of the LTG ratio). Such global GABAergic alterations may be linked to the reductions in functional connectivity observed across the networks. When considering the LTG ratio, significant reductions in $GABA_A$ BP_{ND} remained only in the SACC (and not in the other regions and networks). This suggests that $GABA_A$ BP_{ND} in the SACC is reduced in a regionally specific manner not shared by the rest of the brain. Importantly, it is this region that shows a particular relevance for predicting the recovery of consciousness.

Limitations and Future Directions

The modestly sized and clinically somewhat heterogeneous sample must be mentioned. Although the current data must be considered preliminary, the results are consistent with a prior study showing reduced $GABA_A$ receptor density in nine acute DoC patients [Rudolf et al., 2000]. Furthermore, FMZ PET is a well-developed method that gives stable and reliable results [Salmi et al., 2008]. However, it is necessary to replicate our results in larger and more homogeneous samples. A second limitation is that only one patient could be scanned successfully after recovery. This leaves open interesting questions as to how $GABA_A$ BP_{ND} may change in line with behavioral improvement. Similarly, the rescanning of patients who do not improve would provide information as to whether irreversible brain damage in these patients remains unchanged or gets worse. Future studies may seek to include a brain-lesioned group who retain full consciousness to act as a control for the effect of focal brain injury itself. Moreover, it may be advisable to investigate recovery over periods longer than 3 months. Finally, fluorodeoxyglucose (FDG) PET values have previously been shown to be correlated with [^{11}C]flumazenil PET [Rudolf et al., 2002]. FDG is a more commonly used tracer in DoC patients [Stender et al., 2014] and so it would be interesting to establish if this method can be used in place of FMZ to make clinical outcome predictions by applying an analogous methodology to that described here.

In conclusion, although preliminary, our study demonstrates for the first time that $GABA_A$ receptor binding in the whole brain, and in the SACC particularly, predicts behavioral improvement in DoC. This complements recent clinical reports of therapeutic efficacy of the GABAergic drug Zolpidem in these patients.

ACKNOWLEDGMENTS

The authors have no conflict of interest. The authors thank Dr. Ben Deen for providing the anterior insula template.

REFERENCES

Brefel-Courbon C, Payoux P, Ory F, Sommet A, Slaoui T, Raboyeau G, Lemesle B, Puel M, Montastruc JL, Demonet JF, Cardebat D (2007): Clinical and imaging evidence of zolpidem effect in hypoxic encephalopathy. Ann Neurol 62:102–105.

Chatelle C, Thibaut A, Gosseries O, Bruno MA, Demertzi A, Bernard C, Hustinx R, Tshibanda L, Bahri MA, Laureys S (2014): Changes in cerebral metabolism in patients with a minimally conscious state responding to zolpidem. Front Hum Neurosci 8:917.

Ciurleo R, Bramanti P, Calabro RS (2013): Pharmacotherapy for disorders of consciousness: Are 'awakening' drugs really a possibility? Drugs 73:1849–1862.

Clauss RP (2010): Neurotransmitters in coma, vegetative and minimally conscious states, pharmacological interventions. Med Hypotheses 75:287–290.

Clauss RP (2011): Neurotransmitters in disorders of consciousness and brain damage. Med Hypotheses 77:209–213.

Clauss R, Nel W (2006): Drug induced arousal from the permanent vegetative state. NeuroRehabilitation 21:23–28.

Costes N, Dagher A, Larcher K, Evans AC, Collins DL, Reilhac A (2009): Motion correction of multi-frame PET data in neuroreceptor mapping: Simulation based validation. Neuroimage 47: 1496–1505.

Crone JS, Holler Y, Bergmann J, Golaszewski S, Trinka E, Kronbichler M (2013): Self-related processing and deactivation of cortical midline regions in disorders of consciousness. Front Hum Neurosci 7:504.

Deen B, Pitskel NB, Pelphrey KA (2011): Three systems of insular functional connectivity identified with cluster analysis. Cereb Cortex 21:1498–1506.

Demertzi A, Gomez F, Crone JS, Vanhaudenhuyse A, Tshibanda L, Noirhomme Q, Thonnard M, Charland-Verville V, Kirsch M, Laureys S, Soddu A (2014): Multiple fMRI system-level baseline connectivity is disrupted in patients with consciousness alterations. Cortex 52:35–46.

Desikan RS, Segonne F, Fischl B, Quinn BT, Dickerson BC, Blacker D, Buckner RL, Dale AM, Maguire RP, Hyman BT, Albert MS, Killiany RJ (2006): An automated labeling system for subdividing the human cerebral cortex on MRI scans into gyral based regions of interest. Neuroimage 31:968–980.

Devinsky O, Morrell MJ, Vogt BA (1995): Contributions of anterior cingulate cortex to behavior. Brain 118:279–306.

Du B, Shan A, Zhang Y, Zhong X, Chen D, Cai K (2014): Zolpidem arouses patients in vegetative state after brain injury: Quantitative evaluation and indications. Am J Med Sci 347: 178–182.

Duncan N, Gravel P, Wiebking C, Northoff G (2013): Grey matter density and GABAA binding potential show a positive linear relationship across cortical regions. Neuroscience 235: 226–231.

Frey KA, Holthoff VA, Koeppe RA, Jewett DM, Kilbourn MR, Kuhl DE (1991): Parametric in vivo imaging of benzodiazepine receptor distribution in human brain. Ann Neurol 30: 663–672.

Giacino JT, Kalmar K, Whyte J (2004): The JFK coma recovery scale-revised: Measurement characteristics and diagnostic utility. Arch Phys Med Rehabil 85:2020–2029.

Guadagno JV, Jones PS, Aigbirhio FI, Wang D, Fryer TD, Day DJ, Antoun N, Nimmo-Smith I, Warburton EA, Baron JC (2008): Selective neuronal loss in rescued penumbra relates to initial hypoperfusion. Brain 131:2666–2678.

Heiss WD (2012): PET in coma and in vegetative state. Eur J Neurol 19:207–211.

Heiss WD, Herholz K (2006): Brain receptor imaging. J Nucl Med 47:302–312.

Huang Z, Dai R, Wu X, Yang Z, Liu D, Hu J, Gao L, Tang W, Mao Y, Jin Y, Wu X, Liu B, Zhang Y, Lu L, Laureys S, Weng X, Northoff G (2013): The self and its resting state in consciousness: An investigation of the vegetative state. Hum Brain Mapp 35:1997–2008.

Laureys S, Schiff ND (2012): Coma and consciousness: Paradigms (re)framed by neuroimaging. Neuroimage 61:478–491.

Laureys S, Faymonville ME, Moonen G, Luxen A, Maquet P (2000): PET scanning and neuronal loss in acute vegetative state. Lancet 355:1825–1826.

Logan J, Fowler JS, Volkow ND, Wang GJ, Ding YS, Alexoff DL (1996): Distribution volume ratios without blood sampling from graphical analysis of PET data. J Cereb Blood Flow Metab 16:834–840.

Northoff G (2014): Unlocking the Brain. Volume II: Consciousness. Oxford, New York: Oxford Unviersity Press.

Pistoia F, Mura E, Govoni S, Fini M, Sara M (2010): Awakenings and awareness recovery in disorders of consciousness: Is there a role for drugs? CNS Drugs 24:625–638.

Power JD, Barnes KA, Snyder AZ, Schlaggar BL, Petersen SE (2012): Spurious but systematic correlations in functional connectivity MRI networks arise from subject motion. Neuroimage 59:2142–2154.

Qin P, Di H, Liu Y, Yu S, Gong Q, Duncan N, Weng X, Laureys S, Northoff G (2010): Anterior cingulate activity and the self in disorders of consciousness. Hum Brain Mapp 31:1993–2002.

Qin P, Duncan NW, Wiebking C, Gravel P, Lyttelton O, Hayes DJ, Verhaeghe J, Kostikov A, Schirrmacher R, Reader AJ, Northoff G (2012): GABA(A) receptors in visual and auditory cortex and neural activity changes during basic visual stimulation. Front Hum Neurosci 6:337.

Rodriguez-Rojas R, Machado C, Alvarez L, Carballo M, Estevez M, Perez-Nellar J, Pavon N, Chinchilla M, Carrick FR, DeFina P (2013): Zolpidem induces paradoxical metabolic and vascular changes in a patient with PVS. Brain Inj 27:1320–1329.

Rudolf J, Sobesky J, Grond M, Heiss WD (2000): Identification by positron emission tomography of neuronal loss in acute vegetative state. Lancet 355:115–116.

Rudolf J, Sobesky J, Ghaemi M, Heiss WD (2002): The correlation between cerebral glucose metabolism and benzodiazepine receptor density in the acute vegetative state. Eur J Neurol 9: 671–677.

Saad ZS, Gotts SJ, Murphy K, Chen G, Jo HJ, Martin A, Cox RW (2012): Trouble at rest: How correlation patterns and group differences become distorted after global signal regression. Brain Connect 2:25–32.

Salmi E, Aalto S, Hirvonen J, Langsjo JW, Maksimow AT, Oikonen V, Metsahonkala L, Virkkala J, Nagren K, Scheinin H (2008): Measurement of GABAA receptor binding in vivo with [11C]flumazenil: A test-retest study in healthy subjects. Neuroimage 41:260–269.

Salva P, Costa J (1995): Clinical pharmacokinetics and pharmacodynamics of zolpidem. Therapeutic implications. Clin Pharmacokinet 29:142–153.

Schiff ND (2010): Recovery of consciousness after brain injury: A mesocircuit hypothesis. Trends Neurosci 33:1–9.

Shulman RG, Hyder F, Rothman DL (2003): Cerebral metabolism and consciousness. C R Biol 326:253–273.

Singh R, McDonald C, Dawson K, Lewis S, Pringle AM, Smith S, Pentland B (2008): Zolpidem in a minimally conscious state. Brain Inj 22:103–106.

Song XW, Dong ZY, Long XY, Li SF, Zuo XN, Zhu CZ, He Y, Yan CG, Zang YF (2011): REST: A toolkit for resting-state functional magnetic resonance imaging data processing. PLoS One 6:e25031.

Stender J, Gosseries O, Bruno MA, Charland-Verville V, Vanhaudenhuyse A, Demertzi A, Chatelle C, Thonnard M, Thibaut A Heine L, Soddu A, Boly M, Schnakers C, Gjedde A, Laureys S (2014): Diagnostic precision of PET imaging and functional MRI in disorders of consciousness: A clinical validation study. Lancet 384:514–522.

Thonnard M, Gosseries O, Demertzi A, Lugo Z, Vanhaudenhuyse A, Bruno MA, Chatelle C, Thibaut A, Charland-Verville V, Habbal D, Schnakers C, Laureys S (2013): Effect of zolpidem in chronic disorders of consciousness: A prospective open-label study. Funct Neurol 28:259–264.

Van Dijk KR, Sabuncu MR, Buckner RL (2012): The influence of head motion on intrinsic functional connectivity MRI. Neuroimage 59:431–438.

van Velden FH, Kloet RW, van Berckel BN, Buijs FL, Luurtsema G, Lammertsma AA, Boellaard R (2009): HRRT versus HR+ human brain PET studies: An interscanner test-retest study. J Nucl Med 50:693–702.

Vanhaudenhuyse A, Noirhomme Q, Tshibanda LJ, Bruno MA, Boveroux P, Schnakers C, Soddu A, Perlbarg V, Ledoux D, Brichant JF, Moonen G, Maquet P, Greicius MD, Laureys S, Boly M (2010): Default network connectivity reflects the level of consciousness in non-communicative brain-damaged patients. Brain 133:161–171.

Whyte J, Rajan R, Rosenbaum A, Katz D, Kalmar K, Seel R, Greenwald B, Zafonte R, Demarest D, Brunner R, Kaelin D (2014): Zolpidem and restoration of consciousness. Am J Phys Med Rehabil 93:101–113.

Yamauchi H, Kudoh T, Kishibe Y, Iwasaki J, Kagawa S (2005): Selective neuronal damage and borderzone infarction in carotid artery occlusive disease: A 11C-flumazenil PET study. J Nucl Med 46:1973–1979.

Yan CG, Craddock RC, He Y, Milham MP (2013): Addressing head motion dependencies for small-world topologies in functional connectomics. Front Hum Neurosci 7:910.